Title

Regulation of Adaptive Immunity by the Fractalkine Receptor during Autoimmune Inflammation

Journal

The Journal of Immunology, 191(3)

ISSN

0022-1767

Authors

Garcia, Jenny A
Pino, Paula A
Mizutani, Makiko
et al.

Publication Date

2013-08-01

DOI

10.4049/jimmunol.1300040

Peer reviewed

Published in final edited form as:
J Immunol. 2013 August 1; 191(3): 1063–1072. doi:10.4049/jimmunol.1300040.

Regulation of adaptive immunity by the fractalkine receptor during autoimmune inflammation[1]

Jenny A. Garcia[*], **Paula A. Pino**[*], **Makiko Mizutani**[†], **Sandra M. Cardona**[*], **Israel F. Charo**[‡], **Richard M. Ransohoff**[†], **Thomas G. Forsthuber**[*,§], and **Astrid E. Cardona**[*,§]

[*] Department of Biology. The University of Texas at San Antonio, San Antonio, Texas 78249.

[†] Department of Neurosciences, Neuroinflammation Research Center, Lerner Research Institute, Cleveland Clinic, Cleveland, OH 44195

[‡] Gladstone Institute of Cardiovascular Research, San Francisco, CA 94158.

[§] South Texas Center for Emerging Infectious Diseases, The University of Texas at San Antonio, San Antonio, Texas 78249.

Abstract

Fractalkine, a chemokine anchored to neurons or peripheral endothelial cells, serves as an adhesion molecule or as a soluble chemoattractant. Fractalkine binds CX3CR1 on microglia and circulating monocytes, dendritic cells and NK cells. The aim of this study is to determine the role of CX3CR1 in the trafficking and function of myeloid cells to the central nervous system (CNS) during experimental autoimmune encephalomyelitis (EAE). Our results show that in models of active EAE *Cx3cr1*$^{-/-}$ mice exhibited more severe neurological deficiencies. Bone marrow chimeric mice confirmed that CX3CR1-deficiency in bone marrow enhanced EAE severity. Notably, CX3CR1 deficiency was associated with an increased accumulation of CD115^{+}Ly6C^{-}CD11c^{+} dendritic cells into EAE affected brains which correlated with enhanced demyelination and neuronal damage. Furthermore, higher IFN-γ and IL-17 levels were detected in cerebellar and spinal cord tissues of CX3CR1-deficient mice. Analyses of peripheral responses during disease initiation revealed a higher frequency of IFN-γ and IL-17 producing T cells in lymphoid tissues of CX3R1-deficient as well as enhanced T cell proliferation induced by CX3CR1-deficient DCs. In addition, adoptive transfer of MOG_{35-55} reactive wild type T cells induced substantially more severe EAE in CX3CR1-deficient recipients when compared to wild type recipients. Collectively, the data demonstrate that besides its role in chemoattraction, CX3CR1 is a key regulator of myeloid cell activation contributing to the establishment of adaptive immune responses.

Keywords

EAE/MS; chemokines; dendritic cells; monocytes/macrophages; neuroimmunology; autoimmunity

[1]This research was supported in part by funds from the US National Multiple Sclerosis Society [RG3701 to TGF, and TA 3021 A1/T to AEC] and The National Institutes of Health [NS-52177 to TGF and SC1GM095426 to AEC].

Address for Correspondence Astrid E. Cardona, PhD One UTSA Circle Margaret Batts Tobin Laboratory MBT 1.216 San Antonio, TX 78249 Tel: (210) 458-5071 Fax:(210) 458-5029 astrid.cardona@utsa.edu.

Introduction

Multiple sclerosis (MS) is a chronic, inflammatory demyelinating disease of the CNS causing significant neurological disability in young adults. Supported by experimental evidence largely collected from its major model, experimental autoimmune encephalomyelitis (EAE), MS is considered for many in the field a predominantly T cell-mediated autoimmune disease. Although, the exact cause of MS remains unsolved, CNS inflammation is a key component of the pathophysiology of MS. While chemokines are known to promote tissue inflammation via recruitment of immune cells to these sites, recently it was shown that chemokine-chemokine receptors also participate in cellular activation and modulate effector functions of certain immune cell subsets (1,2).

The discovery of the chemokine receptor CX3CR1 and its unique ligand fractalkine (CX3CL1) in the mid 1990's represented a major advancement in the understanding of myeloid cell function (3-5). Fractalkine is a distinct chemokine, expressed as a membrane bound glycoprotein on neurons and peripheral endothelial cells (3,6,7). The fractalkine receptor (CX3CR1) is present on microglia and circulating monocytes, dendritic cells and NK cells. Fractalkine, first known as neurotactin due to its abundant expression in the brain, plays different roles in different tissue compartments and disease states. We discovered that CX3CL1 signaling promotes microglial survival and controls microglial neurotoxicity through its unique receptor CX3CR1 under certain neurodegenerative and inflammatory conditions. Importantly, in humans two single nucleotide polymorphisms give rise to four allelic receptor variants. The most studied forms are CX3CR1$^{V249/T280}$ (also considered as the reference receptor), and the variant alleles CX3CR1$^{I249/T280}$ and CX3CR1$^{I249/M280}$ present in 20-30% of the population. These changes decrease fractalkine affinity and correlate with enhanced susceptibility to age-related macular degeneration (8,9) and protection from atherosclerosis (10-12). Notably, a genetic study in a Serbian population (397 MS patients) found a significantly lower frequency of the CX3CR1$^{I249/T280}$ haplotype in secondary progressive compared to relapsing-remitting patients. Therefore, understanding the function of CX3CR1 during disease initiation will be valuable to understand the immune pathology of MS.

Monocytes and dendritic cells (13-15), are critical mediators of innate and adaptive immune responses. Notably, CX3CR1 distinguished a monocyte subset in peripheral blood so called “resident” and phenotypically recognized as LFA-1^{+}/LSel^{-}/Ly6C^{-}/CCR2^{-}/CX3CR1^{Hi}, whereas the MCP-1 (Or CCL2) receptor CCR2, marked “inflammatory” monocytes distinguished as LFA-1^{-}/L-Sel^{+}/Ly6C^{+}/CCR2^{+}/CX3CR1^{Lo} (14,16,17). The recent characterization of red fluorescent protein (RFP)-CCR2 knock in mice and the generation of mouse models carrying CX3CR1-GFP/CCR2-RFP reporter proteins provided additional support for a distinct molecular signature of CX3CR1 and CCR2 during embryonic development (18) and brain inflammation. CCR2 is critical for efficient accumulation of Ly6C^{Hi}/CCR2^{Hi} monocytes to the CNS. Furthermore, microglia in the adult naïve and EAE inflamed CNS were found CX3CR1^{Hi}/CCR2^{-} (19) and similar to the populations described in peripheral blood the EAE brain monocytes also appeared as CCR2^{Hi}CX3CR1^{Lo} or CCR2^{Lo}CX3CR1^{Hi} (19). Due to the contrasting expression of CX3CR1 on the two major monocyte populations we sought to investigate the role of CX3CR1 in accumulation of myeloid cells to the CNS during EAE and its effects on brain pathology. For this we used *Cx3cr1*$^{GFP/GFP}$ (or *Cx3cr1*$^{-/-}$) mice and *Cx3cr1*$^{GFP/GFP}$*Ccr2*$^{+/RFP}$ and controls (*Cx3cr1*$^{+/+}$ and *Cx3cr1*$^{+/GFP}$*Ccr2*$^{+/RFP}$) to characterize myeloid cells in brain and lymphoid tissues at peak of EAE disease and investigate the role of these cells in promoting T cell activation and proliferation. Our results show that *Cx3cr1*$^{-/-}$ mice exhibited more severe neurological signs. Radiation bone marrow chimeric mice confirmed that CX3CR1-deficiency in bone marrow enhanced EAE severity. Notably, CX3CR1 deficiency was associated with an

increased accumulation of $CD115^+/Ly6C^-/CCR2^-$ $CD11c^+$ dendritic cells into EAE affected brains which correlated with enhanced demyelination and neuronal damage. Wild type (WT, *Cx3cr1*$^{+/+}$) infiltrating T cells showed an increased expression of IL-10 when compared to CX3CR1-deficient cells. Furthermore, higher IFN-γ and IL-17 levels were detected in cerebellar and spinal cord tissues of CX3CR1-deficient mice. Analyses of peripheral responses during disease initiation revealed a higher frequency of IFN-γ and IL-17 producing T cells in lymphoid tissues of CX3R1-deficient as well as enhanced T cell proliferation induced by CX3CR1-deficient DCs. Finally, adoptive transfer of MOG_{35-55} reactive wild type T cells induced substantially more severe EAE in CX3CR1-deficient recipients when compared to wild type recipients. Collectively, the data demonstrate that CX3CR1 is not only chemotactic but a key regulator of myeloid cell activation contributing to the establishment of adaptive immune responses.

Materials and Methods

Mice

C57BL/6, *Cx3cr1*$^{GFP/GFP}$ (*Cx3cr1*$^{-/-}$), *Cx3cr1*$^{+/GFP}$*Ccr2*$^{+/RFP}$, and *Cx3cr1*$^{GFP/GFP}$*Ccr2*$^{+/RFP}$ mice were maintained at the Laboratory Animal Resources Unit at The University of Texas at San Antonio. All experiments were performed in accordance with NIH guidelines and approved by The University of Texas at San Antonio Institutional Animal Care and Use Committee. Mice were genotyped by polymerase chain reaction (PCR) using DNA isolated from ear punch biopsies, and chemokine receptor specific primers as previously described (1).

Active EAE induction

Active EAE was induced in mice 8-10 weeks old by subcutaneous immunization with 100 μg of MOG_{35-55} peptide in complete Freund's adjuvant as previously described (18). Mice were weighed and examined daily for EAE signs and scored as follows: (0) no signs of neurological disease, (1) lack of tail tone, (2) abnormal gait, hind limb weakness (2.5) partial hindlimb paralysis, (3) complete hindlimb paralysis, (3.5) ascending paralysis, (4) tetraplegia, (5) death. Mice were sacrificed when they reached a score of 2.5-3.0(1). Mice were sacrificed at disease initiation at 11 days post-immunization (p.i.), at peak of EAE disease (16-21 days p.i.) or 60 days p.i. (chronic phase).

Passive EAE induction

Mice were immunized with 300 μg MOG_{35-55} peptide in CFA. Spleen and lymph nodes were harvested and single mononuclear cell suspensions were prepared 10 days p.i. and cultured in the presence of 20 μg/ml MOG_{35-55} , 20 ng/ml murine rIL-23 (R&D Systems) and 10 μg/ml anti-IFN-γ (R4-6A2, BioXcell) in complete media (20-22). After 3 d incubation, cells were collected, washed in DMEM containing 50μg/mL gentamicin and 20-50 × 10^6 cells were i.p injected into wild-type or *Cx3cr1*$^{-/-}$ recipient mice. A separate aliquot of the isolated cells was subjected to IFN-γ and IL-17 cytokine ELISPOT assays. This was performed on primed T cell from WT and CX3CR1-KO mice, to normalize the number of cells injected per recipient and compare similar number of effector cells per experiment. Prior to injection of Recipients were injected with 200 ng pertussis toxin i.p on the day of cell transfer and 48 h after transfer. Mice were weighed and EAE scored daily.

Generation of bone marrow chimeric mice

Recipient mice (5-6 week old) were irradiated with a dose of 9Gy and allowed to recover overnight before bone marrow reconstitution. Bone marrow cells were isolated from femur and tibia as previously described (1). Briefly, mice were sacrificed by CO_2 asphyxiation

followed by cervical dislocation, flushed bone marrow cells were resuspended in Iscoves media without FBS at 15×10^7 cells/ml. Recipient mice were anesthetized 1-2 min (or until animals loss of righting reflexes) in an induction chamber with oxygen flow rate of 1 liter/min and isofluorane delivery to 3-4%, and $15 – 20 \times 10^6$ cells injected via the retro-orbital sinus in a volume of 100-150 μl. Mice were placed in a clean cage and monitored until righting reflex was gained. Six weeks after reconstitution EAE was induced. Efficiency of engraftment was confirmed by flow cytometry 4 weeks after bone marrow reconstitution by virtue of CD45.1 and CD45.2 congenic markers in donor and recipients respectively.

Isolation of mononuclear cells and Flow Cytometry

Perfused brains and spinal cord tissues were dissected from mice at peak of EAE disease and mononuclear cells separated over discontinuous 70/30% percoll gradients as previously described (23), and cellular pellets resuspended in cell staining buffer (Biolegend, San Diego, CA). Blood for single stained controls was collected from the submandibular vein and RBCs depleted by hypotonic lysis and washed in staining buffer. Isolated cells were incubated on ice for 5 min with anti-mouse CD16/CD32 (clone 2.4G2; BD Pharmingen) to block FcRs and then incubated on ice for 30 min with a mix of fluorochrome-conjugated anti-mouse Abs; CD45-PerCP, APC-Cy7 or APC (Clone 30-F11, BD Pharmingen), CD115-PE (Clone AFS98, eBioscience), CD11b-Pe (Clone M1/70), CD11c-PeCy7 (Clone N418, eBioscience), Ly6CAlexa 647 (Clone ER-MP20, AbD Serotec), CD80-APC (Clone 16-10A1), CD86-PerCP (Clone GL-1), and I-A/I-E-Pacific Blue (Mouse MHC-II Clone M5/114.15.2). After washes, cells were resuspended in 2% paraformaldehyde and analyzed in a LSR-II (BD Biosciences, Franklin Lakes, NJ). Similar analyses were carried out in cell suspensions from lymph node and spleens at 11 days p.i. Lymphoid tissues were passed through a 70 μm nylon mesh and spleen RBCs depleted by hypotonic lysis prior flow cytometry.

To quantify the proportion of resident and infiltrating myeloid cells undergoing cell proliferation CNS mononuclear cells were stained with a mix of CD45-APC(Clone 30-F11) and CD11b-PerCP (Clone M1/70) antibodies for 30 min on ice, fixed with 4% PFA for 30 min and then incubated at RT for 10 min in permeabilization buffer (eBioscience). Cells were then stained with Ki67-V450 (Clone B56) in permeabilization buffer for 20 min, washed, resuspended in 2% PFA and acquired on an LSRII. Flow cytometry data is presented as number or percentage of cells, or as mean fluorescence intensity (MFI) for MHC-II, CD80 and CD86 markers.

Immunohistochemistry staining of brain sections

Following buffer perfusion mice were perfused with 4% PFA. Dissected tissues were post-fixed 24-36 hours in 4% PFA, cryoprotected in 20% glycerol in 80mM phosphate buffer, pH 7.6 for 48 h at 4°C. Free-floating 30 μm sections were prepared using a freezing microtome and stored at -20°C until use (2). After blocking, tissues were stained overnight at 4°C with anti-mouse CD45 antibodies (Clone IBL-3/16, AbD Serotec, Raleigh, NC), anti-mouse NeuN (clone A60, Millipore, Billerica, MA), monoclonal anti-calbindin antibody (Clone C26D12, Millipore) or anti-myelin basic protein (MBP) antibody (Invitrogen). Tissues were then incubated with biotin-labeled secondary antibody, and developed with avidin-biotin peroxidase system (Vector Laboratories, Burlingame, CA) with DAB as a substrate (Invitrogen, Carlsbad, CA). Tissues were then mounted onto super frost plus slides and allowed to air dry and baked at 50°C for 20 min. Slides were then cleared in xylene and mounted using Permount reagent. After tissues were mounted onto slides, sections were stained with anti-CD45 antibodies and subjected to Nissl staining. For this sections were hydrated on graded ethanol solutions (100%, 95% and 70%) and stained for 3 min in 0.5% solution of cresyl violet followed by dehydration (70%, 95% and 100% ethanol). To assess

differences myelin content, 3 tissue sections per mouse (n = 4 per group) were imaged and the area of myelin immunoreactivity in 8 random images per section obtained using Image-Pro Plus 6.2.1 (Media Cybernetics, Inc) in a blinded manner. Similarly, calbindin positive cells were counted in 10 randomly acquired images per section in 3 different tissues per mouse. Individual cells were counted using the count analysis tool in Adobe Photoshop extended CS4 v11 (Adobe, Inc).

T cell proliferation assay

Mice immunized with 300μg MOG_{35-55} in CFA were sacrificed 11 days p.i. T cells were enriched from spleens by magnetic negative selection (Stemcell Technologies). For dendritic cell isolation, spleens were extracted and dissociated in spleen dissociation media (Stemcell Technologies) and enriched for CD11c+ cells (Stemcell Technologies). T cells were labeled with the proliferation dye CFSE (eBioscience) and plated in complete media with 20 μg MOG_{35-55} at 1×10^6 cells per well in a 96 well plate. Either CX3CR1 WT or KO CD11c+ cells were added to the T cells at an equal ratio, then the cells were incubated at 37°C for 3 days. Cells were labeled with viability dye eFluor780 (eBioscience), then blocked with CD16/CD32 (BD Pharmingen) and labeled with a mixture of antibodies for flow cytometrical analysis using LSR II.

Cytokine ELISPOT assay

Mice were immunized with 100μg MOG_{35-55} and sacrificed 11 days p.i. Spleen and lymph nodes were harvested and cells were plated at 1×10^6 per well with 10μg/mL MOG_{35-55} in complete HL-1 serum free media in a 96 well filter plate that was previously sensitized with purified capture anti-IL-17 (Clone 17CK15A5, eBioscience) or anti-IFNγ (Clone AN-18 eBioscience) and blocked with 1× PBS/1% BSA. After 24 hours of incubation at 37°C/ 5% CO_2, the cells were washed with 0.5% Tween-20 in PBS then labeled with biotin anti-IL-17 detection antibodye (Clone eBio17B7) or biotin anti-IFN-γ detection antibody (Clone R4-6A2) and incubated at 4°C ON. The cells were then incubated for 2 hours at room temperature with Streptavidin AP (Invitrogen) diluted in PBS containing 1%BSA/0.5% Tween-20 and developed with BCIP/NBT Phosphatase Substrate (KPL). Plates were read and spots counted using ImmunoSPOT software. Similarly, IFN-γ and IL-17 producing cells were assayed in total brain leukocyte populations (isolated via percoll gradients as described above) from WT and CX3CR1-KO mice at peak of EAE disease. Number of spots in non-stimulated control wells were subtracted from the stimulated well and data is presented as spot forming cells (SFCs) per total million of cells added in the assay.

Quantitative RT-PCR

Tissues were dissected from perfused mice at the peak of EAE disease. Cerebellum was carefully detached using a scalpel and stored separately from forebrain and spinal cord tissues. Total RNA was isolated using Trizol reagent according to the manufacturer's instructions. Quantity was assessed with a Nanodrop 1000 and RNA quality confirmed over 1% agarose gels. RNA was transcribed using TaqMan reverse-transcription reagents. Quantitative real-time PCR was performed with TaqMan Master mix and gene expression assay. Samples were analyzed on an Applied Biosystems 7900HT thermal cycler. All TaqMan reagents were from Applied Biosystems. Reactions were run in triplicates and expression levels were normalized to beta-actin.

Statistical analysis

Data are presented as mean ± SEM. Transcript data for IL-17 was analyzed using ANOVA. For all other experiments, differences between groups were analyzed using an unpaired *t* test

with Graph Pad Prism software (San Diego, CA). *P* values are shown in the data (*) when $P < 0.05$ and > 0.01, and (**) when $P < 0.01$.

Results

Peripheral CX3CR1-deficiency confers more severe EAE

Two mouse models of CX3CR1-deficiency were reported in the earlier 2000s (24,25). In mixed 50:50 hybrids of the C57BL/6 and 129/Sv strains *Cx3cr1*$^{-/-}$ mice upon active immunization with MOG_{35-55} peptides revealed a slightly earlier disease onset (24,26,27). A different study using mutant mice engineered by disrupting the CX3CR1 locus by insertion of the green fluorescence protein (GFP) reporter protein showed that CX3CR1-deficient mice on the *CD1d*$^{+/+}$ and *CD1d*$^{-/-}$ background developed EAE disease with earlier onset and correlated with a selective deficiency of NK cells in the CNS (28). Due to the expression of CX3CR1 by distinct monocyte/macrophage populations (18,19), we sought to extend these studies and characterize the myeloid compartment in the CNS during EAE in the absence of CX3CR1 signaling. To begin to address this issue, active EAE was induced in *Cx3cr1*$^{GFP/GFP}$ (*Cx3cr1*$^{-/-}$, KO) mice backcrossed to the C57BL/6J background for >14 generation and WT littermates via subcutaneous injection of 100 μg MOG_{35-55} peptide and the mice were observed for EAE disease. All mice developed signs of EAE (Figure 1A). However, CX3CR1-deficient mice showed EAE signs at an earlier time point (Figure 1B). The peak of disease was also manifested earlier in *Cx3cr1*$^{-/-}$ mice (Figure 1B) and the EAE signs were significantly more severe in the absence of CX3CR1, as shown by the comparison of maximum EAE scores between the groups (Figures 1A and 1C). To delineate the contribution of peripheral versus CNS resident cells to disease progression we generated radiation bone marrow chimeric mice and active EAE was induced and monitored as described earlier. Reconstitution of both WT or *Cx3cr1*$^{-/-}$ recipient mice with *Cx3cr1*$^{-/-}$ bone marrow (KO → WT and KO → KO) showed a severe and non-remitting form of EAE, with a high proportion of mice exhibiting ascending paralysis that was sustained up to 45-50 days p.i. (Figure 1D, E). Peak EAE was comparable in WT → KO and KO → WT chimeric mice (Figure 1D), however recipients of KO bone marrow failed to recover from EAE , whereas recipients of WT bone marrow (WT → KO) exhibited a progressive recovery and motor function was regained in both hind limbs. Control bone marrow chimeric mice (WT→ WT and KO→KO, Figure 1 E) showed a similar EAE phenotype in which the genotype of the circulating bone marrow derived cells correlates with neurological disease as observed in the mixed chimeric mice (Figure 1D). Overall the results show that EAE severity observed in CX3CR1-deficient mice was due to absence of fractalkine signaling on peripheral bone marrow derived cells.

Increased severity of CNS pathology in CX3CR1-deficient mice correlates with the increased accumulation of dendritic cells in the CNS

To investigate the mechanism underlying the increased severity of EAE in the absence of CX3CR1 signaling, we examined CNS inflammation at the time of peak disease in CX3CR1-KO mice also carrying the CCR2-RFP reporter protein. Heterozygous mice with normal receptor function (*Cx3cr1*$^{+/GFP}$*Ccr2*$^{+/RFP}$) and CX3CR1-deficient mice carrying the CCR2-RFP reporter (*Cx3cr1*$^{GFP/GFP}$ *CCR2*$^{+/RFP}$) were investigated for the accumulation of monocyte subsets upon active EAE induction (Figures 2A and 2B). Myeloid subsets in the CNS were distinguished by flow cytometry using antibodies against CD45 to distinguish $CD45^{Hi}$ infiltrating leukocytes from $CD45^{Lo}$ microglial cells. $CD45^{Hi}$ cells were further analyzed for the monocyte marker CD115 expression and $CD115^{+}$ cells for Ly6C and CD11c expression. The results show that in heterozygous mice, more than 85% of $CD115^{+}$ monocyte-lineage cells were $Ly6C^{Hi}$ (also $CCR2^{Hi}$ by virtue of RFP-expression), indicating a predominant infiltration of this population to the CNS during EAE demonstrating the

importance of CCR2 for recruitment of this subset into the CNS. In contrast, accumulation of the $Ly6C^{Lo}$ population was dramatically increased in the absence of CX3CR1 (Figure 2B) and 60% of these cells also expressed the CD11c marker characteristic of dendritic cells. The population of $Ly6C^{-}CD11c^{+}$ cell expressed CX3CR1 as revealed by comparison of CX3CR1-GFP and CCR2-RFP fluorescence intensities in the various myeloid populations. $Ly6C^{Lo}$ cells expressed higher levels of CX3CR1 than $Ly6C^{Hi}$ cells (Figure 2C, P=0.008 for comparison of CX3CR1-GFP expression between $Ly6C^{+}CD11c^{+}$ and $Ly6C^{-}CD11c^{+}$ cells, P=0.016 for comparison of CCR2-RFP between $Ly6C^{+}CD11c^{+}$ and $Ly6C^{-}CD11c^{+}$ groups. P =0.046 for comparison of CX3CR1-GFP and CCR2-RFP expression within $Ly6C^{+}CD11c^{+}$ population and P =0.008 for comparison of CX3CR1-GFP and CCR2-RFP expression within $Ly6C^{-}CD11c^{+}$ population). These results suggest that $Ly6C^{Hi}/CCR2^{+}$ and $Ly6C^{Lo}/CX3CR1^{+}$ subsets represent distinct populations with specialized functions within the CNS.

To establish a relationship between the infiltration of myeloid cells and CNS pathology, brains were sectioned and analyzed at the peak of EAE by immunohistochemistry. Tissues were stained with antibodies against CD45, as a generalized marker of inflammation (Figure 2D-F), MBP to assess demyelination (Figure 2G-I) and calbindin as a marker for Purkinje cells in cerebellar regions (Figure 2J-L). When compared to naïve CX3CR1-KO tissues, (Figure 2D) infiltration of peripheral cells was evident in diseased WT mice (Figure 1E) and CX3CR1-KO tissues. However, CD45 immunoreactivity was found most dramatic in forebrain and cerebellar white matter of CX3CR1-KO mice (Figure 2F and Supplementary Figure 1 and 2). Myelin staining revealed a defined pattern in naïve (Figure 2G) and diseased WT mice (Figure 2H), with myelin fibers darkly stained and axons easily visualized. In WT tissues affected by EAE, strong myelin immunoreactivity is observed in areas close to inflammatory cuffs (Figure 2H). In contrast, CX3CR1-KO tissues revealed a decreased intensity in the myelin staining; axons appeared thinner and shorter, and less defined axons were visualized in the cerebellar region (Figures 2I). Purkinje cells were detected along the granular cell layer of naïve mice (Figure 2J) and diseased WT mice (Figure 2K). In contrast, in CX3CR1-KO mice calbindin positive neurons appeared with an altered morphology. Deteriorated/degenerating cells were evident by the presence of a disrupted lining of the granular cell layer and ovoids at the ends of the axons were clearly visualized (Figure 2L and Supplementary Figure 1). Quantification of myelin immunoreactive area shows that naïve CX3CR1-KO mice do not differ from naïve WT mice (Figure 2M). Similar results were found when assessing the number of calbindin positive neurons (Figure 2N). However, upon EAE induction a reduction in both myelin (Figure 2M, *P=0.03 between WT naïve and WT-EAE groups, P= 0.0002 between KO naïve and KO-EAE groups, and **P<0.0001 between WT-EAE and KO-EAE groups) and neuronal counts were detected with CX3CR1-KO mice revealing an more dramatic reduction when compared to diseased WT mice (Figure 2N, *P=0.04 between WT-EAE and KO-EAE and P=0.021 between KO naïve and KO-EAE groups). Therefore, the results indicate that an increased inflammatory reaction, dominated by a myeloid subset with a $CD115^{+}Ly6C^{Lo}CD11c^{+}$ phenotype, correlated with enhanced demyelination and neuronal damage in CX3CR1-KO mice.

Differential cytokine expression in CX3CR1-KO mice is indicative of an increased pro-inflammatory environment in the CNS

To further examine mechanisms by which this myeloid subset conferred CNS pathology we sought to investigate the frequency of IFN-γ and IL-17 MOG_{35-55} specific producing T cells in the periphery. For this we utilized lymph nodes and spleen tissues from actively immunized WT and CX3CR1-KO mice in ELISPOT assays performed at 11 and 60 days p.i. The results show that during disease initiation IFN-γ antigen specific producing T cells

were detected in higher frequency in lymph node tissues (Figure 3A). IL-17 producing T cells were significantly abundant in both lymph nodes (Figure 3A) and spleen tissues of CX3CR1-KO mice (Figure 3B) when compared to WT mice at 11 days p.i. By day 60 p.i. the frequency of antigen specific T cells producing IFN-γ or IL-17 was undetectable in lymph nodes (data not shown). However, in the spleen both WT and KO mice revealed IFN-γ producing cells in comparable frequencies. In addition, the frequency of IL-17 producing T cells was higher in CX3CR1-deficient mice when compared to WT mice, with a notable decrease at 60 days p.i. (Figure 3B). The results suggest that CX3CR1-KO mice exhibited increased numbers of peripheral IL-17 secreting antigen specific T cells. Due to the differential inflammatory response visualized by tissue immunohistochemistry, cytokine expression was also assessed in the CNS by qRT-PCR and analyzed separately in forebrain, cerebellum and spinal cord regions. Compared to WT mice, CX3CR1-KO mice exhibited increased mRNA transcript expression of IFN-γ in cerebellar and spinal cord tissues (Figure 3C) and increase in IL-17 was revealed in forebrain and cerebellar regions (Figure 3D, $*P = 0.005$). The anti-inflammatory cytokine IL-10 was detected at significantly higher levels in spinal cord tissues of WT mice (Supplementary Figure 3A, $**P = 0.0008$), whereas in all CNS tissues of CX3CR1-deficient mice TNF-α levels where higher when compared to diseased WT mice (Supplementary Figure 3B). Cytokine ELISPOT assays (Figure 3E) using total brain leukocyte populations at peak of EAE disease revealed a significantly increase in the number of IL-17 producing cells from CX3CR1-KO mice and a higher ratio of IL-17/IFN-γ SFCs when compared to WT mice (Figure 3F, *P<0.05). Overall our results suggest an important role for CX3CR1/CX3CL1 in the regulation of antigen presenting cell effector function and in turn in the modulation of the development of a pro-inflammatory environment.

Effect of CX3CR1-deficiency on antigen presenting cell effector function

To address the role of CX3CR1 on dendritic cells and their effects to modulate T cell function we performed in vitro proliferation assays using MOG_{35-55} primed T cells isolated from actively immunized WT mice at day 11 p.i. T cells were then mixed with WT or *Cx3cr1*$^{-/-}$ APCs (CD11b+CD11c+) isolated from spleens and lymph nodes or from diseased brains and dilution of the proliferation dye on T cells evaluated. Cultured cells were stained with the viability dye eFluor780 (Figure 4A) and only live CD4+ T cells were analyzed (Figure 4B). Cultures containing WT dendritic cells (Figure 4C and 4D) revealed less proliferating T cells when compared to cultures containing CX3CR1-KO peripheral dendritic cells (Figures 4C and D). A similar result was obtained when using CNS derived myeloid cells (Supplementary Figure 4). To further address the role of CX3CR1 on adaptive immunity via modulation of myeloid cell function, we examine expression of class II histocompatibility antigens I-A^b and the costimulatory molecules CD80 and CD86 in spleen and LN myeloid cells (Figure 5A and 5C) from actively immunized mice at 11 days p.i. and from brain leukocyte populations at peak of EAE disease (Figure 5B and 5D). The proportions of myeloid subsets $CD11b^+Ly6C^+CD11c^+$ and $CD11b^+Ly6C^-CD11c^+$ in spleen and lymph nodes of actively immunized mice were comparable between WT and CX3CR1-KO mice. However, CX3CR1-KO cells exhibited increased surface expression of MHC-II (Figure 5A, $*P = 0.03$). Similarly, CD11c+ cells isolated from inflamed CX3CR1-KO brains showed increased surface expression of MHC-II and CD86 when compared to WT mice. Notably, in the brain the $CD45^{Hi}CD11c^+$ population predominates in MHC-II expression when compared to the $CD45^{Lo}CD11b^+$ microglia population or to the infiltrating myeloid cell population that is CD11c-negative (Figure 5B, $*P<0.05$). Interestingly CD86 expression was found upregulated in all CX3CR1-KO myeloid populations not only in lymphoid tissues (Figure 5C), but also in the brain including microglia, and infiltrating $CD11b^+CD11c^-$ and $CD11b^+CD11c^+$ populations (Figure 5D, $*P<0.05$).

To assess differences in the proliferation of the CNS myeloid cells, we performed flow cytometry on cells isolated from diseased WT (Figure 6A and B) and KO (Figures 6C and D) brains. The cells were stained with antibodies against CD45, CD11c, CD11b and the proliferation marker Ki67. CX3CR1-KO mice exhibited a higher proportion of Ki67+ myeloid cells that included the $CD45^{Lo}CD11b^{+}$ microglia and $CD45^{Hi}CD11b^{+}CD11c^{+}$ infiltrating dendritic cells (Figure 6C). Altogether the results indicate that CX3CR1 plays an important role in modulating the activation of peripheral and CNS antigen presenting cells.

CX3CR1 modulates EAE severity via regulation of APC cell function

To strengthen the previous results we investigated the role of CX3CR1 on the effector phase of EAE by comparing disease course after adoptive transfer of WT T cells or KO T cells in WT and KO recipients (Figure 7). Given the fact that the frequencies of IFN-γ and IL-17 producing T cells was higher (almost 3X fold) in KO mice upon induction of EAE via active immunization, donor T cells for adoptive transfer experiments were analyzed by ELISPOT assays for IFN-γ and IL-17 to determine the overall numbers of effector cells elicited. The numbers of cells to be injected for the adoptive transfer experiments were adjusted to reflect similar proportions of IFN-γ and IL-17 producing cells in both donor WT and KO T cells. The data indicated that MOG_{35-55} primed *Cx3cr1*$^{-/-}$ (Figures 7A and 7B) or *Cx3cr1*$^{+/+}$ T cells (Figures 7A, C and D) induced a similar EAE phenotype as shown by the maximum EAE score in the four experimental groups analyzed. From 4 different experiments analyzed, the incidence of EAE was higher in the KO recipients with about 80% of mice displaying neurological signs. EAE manifestations were more severe in *Cx3cr1*$^{-/-}$ recipient regardless of the genotype of the T cells used for the passive transfer of EAE.

Discussion

The diversity and polarization capacity of the myeloid cells including microglia, monocytes, macrophages and dendritic cells, has introduced a challenge to understand the function of the myeloid lineage during conditions that involve microbial pathogens, autoimmune inflammation or neurodegeneration (29). In general the mononuclear phagocyte system plays an important role in development, scavenging, inflammation and antimicrobial defenses. However, cell signaling pathways elicited in response to extracellular signals guides the development of distinct population of myeloid cells (30). Main subsets of blood monocytes that have been studied in mice can be distinguished on the basis of Ly6C/CCR2/CX3CR1 expression. Inflammatory $Ly6C^{+}/CCR2^{Hi}/CX3CR1^{Lo}$ murine monocytes are believed to the recruited from blood to tissues following infection where they undergo activation and their response appear to be pathogen dependent. On the other hand $Ly6C^{-}/CCR2^{Lo}/CX3CR1^{Hi}$ monocytes appear to populate normal tissues and exhibit long-range crawling over the endothelium of capillaries, small veins and arteries, a process that may be involved in surveillance. $Ly6C^{-}$ monocytes are suggested to be involved in tissue repair but a role in regulating T-cell function is not yet described. It has also been defined that a fraction of murine monocytes exhibit suppressor functions and can be found in the spleen or liver of mice and inhibit T-cell proliferation. In humans $CD14^{+}$ monocytes that consist of $CD16^{+}$ and $CD16^{-}$ cells resemble $Ly6C^{+}$ murine monocytes. In contrast, murine patrolling $Ly6C^{-}$ monocytes are more similar to the human $CD14^{Lo}$ subset (13). Although the heterogeneity of monocytes is complex, current data supports the notion that $Ly6C^{+}/CCR2^{Hi}/CX3CR1^{Lo}$ and $Ly6C^{-}/CCR2^{Lo}/CX3CR1^{Hi}$ commit to differentiate more readily into M1-like and M2-like inflammatory monocytes or DCs respectively (30).

The fractalkine receptor, CX3CR1 plays neuroprotective roles in selected CNS pathologies including the CX3CR1-SOD^{G93A} transgenic mouse model of ALS. Also, the absence of CX3CR1 led to increased levels of IL-1β and enhanced neuronal damage after peripheral lipopolysaccharide administration in a model of low level endotoxemia (2). In addition,

CX3CR1-deficient mice exhibited an increased loss of tyrosine-hydroxylase-positive neurons in the substantia nigra pars compacta (SNpc) after acute MPTP intoxication, which correlated with robust microglial activation. However, no effect on striatal dopaminergic contenta was observed when *Cx3cr1*$^{-/-}$ mice were treated with methamphetamine (31). Also during EAE, CX3CR1 appears to be protective (28) by affecting the accumulation of NK cells to CNS tissues, but the role of CX3CR1 in myeloid cell trafficking and function has not been addressed. Fractalkine, the sole CX3CR1 ligand, displays properties of both chemokines and adhesion molecules, acting as a chemoattractant for cells expressing the receptor and mediating high affinity adhesion when membrane-tethered fractalkine interacts with CX3CR1^{+} monocytes. The neuroprotective function of CX3CL1 was first reported in hippocampal neurons via CX3CR1 blockade in vitro (32). In an excitotoxic model of neuronal death, CX3CL1 promoted survival of hippocampal neurons and CX3CL1-mediated microglial release of adenosine contributed to neuronal protection via upregulation of neuronal adenosine receptor AR1 (33,34). Conversely, CX3CR1 blockade was associated with smaller infarct size and enhanced recovery in a model of focal cerebral ischemia (35). From these studies, blocking CX3CL1 signaling seemed to be deleterious during CNS inflammation.

We have identified an important role of CX3CR1 for antigen presenting cell effector function in mouse models of MS. CX3CR1-expressing mice exhibit Ly6C^{Hi}CX3CR1^{Lo} monocytes that control the inflammatory lesions (19), whereas in absence of CX3CR1 the inflammatory reaction in the CNS is dominated by a population of dendritic cells that is CD11b^{+}Ly6C^{-}CD11c^{+}CX3CR1^{Hi}. Therefore, CX3CR1-deficient mice provide a novel model to further characterize these cells under various chronic inflammatory settings. This population showed increased expression of markers of antigen presentation and co-stimulation, induced T cell proliferation, and the affected CNS correlated with a predominance of IL-17 producing cells (Figures 3D and 3F). The mechanism linking CX3CL1/CX3CR1 interaction to modulation of antigen presentation and costimulation is under current investigation. The involvement of fractalkine signaling and regulation of the master MHC-II regulator CIITA is a likely target as well as several STAT molecules. We have evidence that myeloid cells from CX3CL1 (ligand) deficient mice upon LPS stimulation exhibit upregulation of MHC-II, and addition of recombinant mouse fractalkine decreased MHC-II expression on both CD11c+ and CD11cmyeloid cell populations (Garcia et al, unpublished findings). Therefore, defining the players in this signaling pathway is the next step to further our understanding of the neuroprotective effects of fractalkine during autoimmune inflammation.

Overall the findings our studies are of great relevance due to the implication of the human polymorphic variants (V249I and T280M) in altering fractalkine-receptor binding affinity (12) as well as expression level of CX3CR1 (9). The association of the variant receptor with chronic inflammatory diseases including Crohn's disease (36), atherosclerosis and coronary artery disease (10,12,37) has been demonstrated. Importantly, protective roles in atherosclerosis and acute coronary events have been suggested (38,39), contrasting an association to increased susceptibility to age reacted macular degeneration. The decreased binding of the variant receptors to the ligand CX3CL1 on peripheral endothelial cells may explain the protective effects in settings of peripheral inflammation. However, little is known about the association of human CX3CR1 variants in in CNS conditions. From our data in experimental mice with defective CX3CR1 signaling, we argue that abnormal CX3CR1-CX3CL1 interactions will be deleterious due to increased influx of highly activated myeloid populations that might potentially enhance and sustain T cell responses within the CNS. A genetic analysis of MS patients revealed significantly lower frequency of the CX3CR1$^{I249/T280}$ haplotype in secondary progressive patients when compared to relapsing-remitting patients (40). Therefore, there is a possible protective effect of the

reference I249 allele on SP MS when linked with T280. Findings in MS patients added to our results show that CX3CR1-deficiency alters not only the NK cell compartment but also myeloid cell lineage and potentially microglial cells and additional human studies should be directed to identify possible associations of these polymorphic variants with CNS inflammation. The results presented showed that absence of CX3CR1 correlated with enhanced brain inflammation and more severe EAE neurological signs. Reconstitution of WT recipients with CX3CR1-deficient bone marrow revealed that peripheral CX3CR1 has a profound effect in CNS inflammation as a more severe neurological disease developed in these mice. The pathology in the CX3CR1-deficient mice showed that the inflammatory reaction correlated with more demyelination and neuronal damage. To further investigate mechanisms that lead to differences in myelin density between WT and CX3CR1-deficient mice, we compared Olig2 and ciliary neurotrophic factor (CNTF) expression by immunohistochemistry in brain sections from WT and KO mice at peak disease (unpublished data). Olig2+ cells appear increased in cerebellar areas of EAE affected CX3CR1-KO mice when compared to WT mice. Expression of CNTF was abundant in cerebellar regions of naïve and EAE WT mice but was reduced in diseased KO mice. Therefore, we hypothesize that CX3CR1-KO mice exhibit a defect in demyelination. How the inflammatory reaction contributes to modulation of CNTF expression is still under investigation.

Comparison of myeloid cell subsets showed an enrichment of monocyte derived (CD115+) $Ly6C^{-}$CD11c+ dendritic cells in the EAE brain. Although $Ly6C^{-}$ monocytes migrate to CNS under steady-state conditions, they do no tend to home to sites of inflammation. However, our data showed that in absence of CX3CR1-signaling this particular $Ly6C^{-}$CD11c+ subset more readily infiltrates the inflamed brain where it undergoes proliferation and may play an important role in sustaining encephalitogenic T cell responses. We focused our studies on investigating the role of CX3CR1 for APC function including modulation of costimulatory molecules and MHC-II presentation, and found that CX3CR1-deficient APCs showed a higher expression of molecules involved in T cell co-stimulation. In humans, immunosenescence has been associated with the peripheral expansion of a population of $CD4+CD28^{-}$ T cells. In MS patients this particular subset exhibited a cytotoxic phenotype and CX3CR1 discriminated these cells from their $CD4^{+}CD28^{+}$ counterparts. Importantly, CD4+CD28+ T cells accumulate in MS lesions of a subgroup of patients, but their exact contribution of CX3CR1 in the modulation of the cytotoxic phenotype is uncertain (41). The role of CX3CR1 on murine T cells has not been explored as only a small percentage of peripheral T cells express CX3CR1. We are currently addressing inflammatory conditions that may trigger upregulation of CX3CR1 on T cells and that could subsequently alter effector immune responses. In the present study to address the role of CX3CR1 on T cells we compared adoptive transferred EAE in KO and WT recipients using primed WT or KO T cells. It is important to note that *Cx3cr1*$^{-/-}$ mice elicited a higher frequency of IL-17 producing cells, but we addressed this issue by injecting similar numbers of IL-17 producing cells. Therefore, EAE disease was compared in adoptive transfer settings using equivalent number of encephalitogenic T cells from primed WT or *Cx3cr1*$^{-/-}$ mice. Altogether the adoptive transfer EAE results suggest that CX3CR1-deficieny on T cells does not affect disease severity.

From the cytokine analysis, elevated levels of TNF-α in brain and spinal cord of CX3CR1-KO mice produced by the abundant myeloid population and/or T cells may contribute to the maintenance of the inflammatory reaction within the CNS as previously shown. During EAE TNF has been shown to produce contrasting pathogenic and protective roles in CNS and secondary lymphoid organs respectively. In the CNS, TNF on myeloid cells has been shown to accelerate onset of EAE by regulating chemokine expression (42) and driving recruitment of inflammatory cells to the CNS by acting on the endothelium of the blood brain barrier

(43). TNF can also function by activating microglia and astrocytes (44,45) and promoting upregulation of adhesion molecules (46,47).

Our data supports the notion that CX3CR1 plays neuroprotective roles during EAE and suggest that peripheral CX3CR1 expression restricts trafficking of $Ly6C^{Lo}CX3CR1^{Hi}$ cells to the CNS likely by interaction with the peripherally expressed ligand. As we advance our knowledge in the understanding of myeloid cell subtypes, it is important to clarify whether they arise from a common bone marrow precursor or if they differentiate within particular tissues under the pressures of the surrounding environment to exert specialized functions. CX3CR1, as an inflammatory and regulatory receptor, poses an intriguing biology and its role in the human population under various neuroinflammatory conditions is yet to be determined.

Supplementary Material

Refer to Web version on PubMed Central for supplementary material.

Acknowledgments

We thank Difernando Vanegas (The University of Texas Health Science Center at San Antonio) for assistance in the generation of the bone marrow chimeras, Niannian Ji (The University of Texas San Antonio) for technical assistance with the ELISPOT assay, The RCMI Advanced Imaging Center, and Elizabeth Morris (The University of Texas at San Antonio) for secretarial assistance.

References

1. Cardona AE, Sasse ME, Mizutani M, Cardona SM, Liu L, Savarin C, Hu T, Ransohoff RM. Scavenging roles of chemokine receptors: chemokine receptor deficiency is associated with increased levels of ligand in circulation and tissues. Blood. 2008
2. Cardona A, Pioro EP, Sasse ME, Kostenko V, Cardona SM, Dijkstra IM, Huang D, Kidd G, Dombrowski S, Dutta R, Lee J, Cook DN, Jung S, Lira S, Littman DR, Ransohoff RM. Control of microglial neurotoxicity by the fractalkine receptor. Nat. Neurosci. 2006; 9:917–924. [PubMed: 16732273]
3. Bazan JF, Bacon KB, Hardiman G, Wang W, Soo K, Rossi D, Greaves DR, Zlotnik A, Schall TJ. A new class of membrane-bound chemokine with a CX3C motif. Nature. 1997; 385:640–644. [PubMed: 9024663]
4. Rossi DL, Hardiman G, Copeland NG, Gilbert DJ, Jenkins N, Zlotnik A, Bazan JF. Cloning and characterization of a new type of mouse chemokine. Genomics. 1998; 47:163–170. [PubMed: 9479488]
5. Combadiere C, Salzwedel K, Smith ED, Tiffany HL, Berger EA, Murphy PM. Identification of CX3CR1. A chemotactic receptor for the human CX3C chemokine fractalkine and a fusion coreceptor for HIV-1. Journal of Biological Chemistry. 1998; 273:23799–23804. [PubMed: 9726990]
6. Mizoue LS, Bazan JF, Johnson EC, Handel TM. Solution structure and dynamics of the CX3C chemokine domain of fractalkine and its interaction with an N-terminal fragment of CX3CR1. Biochemistry. 1999; 38:1402–1414. [PubMed: 9931005]
7. Hatori K, Nagai A, Heisel R, Ryu JK, Kim SU. Fractalkine and fractalkine receptors in human neurons and glial cells. J Neurosci. Res. 2002; 69:418–426. [PubMed: 12125082]
8. Tuo J, Smith BC, Bojanowski CM, Meleth AD, Gery I, Csaky KG, Chew EY, Chan CC. The involvement of sequence variation and expression of CX3CR1 in the pathogenesis of age-related macular degeneration. FASEB J. 2004; 18:1297–1299. [PubMed: 15208270]
9. Chan CC, Tuo J, Bojanowski CM, Csaky KG, Green WR. Detection of CX3CR1 single nucleotide polymorphism and expression on archived eyes with age-related macular degeneration. Histol. Histopathol. 2005; 20:857–863. [PubMed: 15944936]

10. Moatti D, Faure S, Fumeron F, Amara M, Seknadji P, McDermott DH, Debre P, Aumont MC, Murphy PM, de Prost D, Combadiere C. Polymorphism in the fractalkine receptor CX3CR1 as a genetic risk factor for coronary artery disease. Blood. 2001; 97:1925–1928. [PubMed: 11264153]
11. Nassar BA, Nanji AA, Ransom TP, Rockwood K, Kirkland SA, Macpherson K, Connelly PW, Johnstone DE, O'Neill BJ, Bata IR, Andreou P, Title LM. Role of the fractalkine receptor CX3CR1 polymorphisms V249I and T280M as risk factors for early-onset coronary artery disease in patients with no classic risk factors. Scand. J. Clin. Lab Invest. 2008; 68:286–291. [PubMed: 18609106]
12. McDermott DH, Fong AM, Yang Q, Sechler JM, Cupples LA, Merrell MN, Wilson PW, D'Agostino RB, O'Donnell CJ, Patel DD, Murphy PM. Chemokine receptor mutant CX3CR1-M280 has impaired adhesive function and correlates with protection from cardiovascular disease in humans. J Clin. Invest. 2003; 111:1241–1250. [PubMed: 12697743]
13. Auffray C, Fogg D, Garfa M, Elain G, Join-Lambert O, Kayal S, Sarnacki S, Cumano A, Lauvau G, Geissmann F. Monitoring of blood vessels and tissues by a population of monocytes with patrolling behavior. Science. 2007; 317:666–670. [PubMed: 17673663]
14. Geissmann F, Jung S, Littman DR. Blood monocytes consist of two principal subsets with distinct migratory properties. Immunity. 2003; 19:71–82. [PubMed: 12871640]
15. Geissmann F, Gordon S, Hume DA, Mowat AM, Randolph GJ. Unravelling mononuclear phagocyte heterogeneity. Nat. Rev. Immunol. 2010; 10:453–460. [PubMed: 20467425]
16. Auffray C, Sieweke MH, Geissmann F. Blood monocytes: development, heterogeneity, and relationship with dendritic cells. Annu. Rev. Immunol. 2009; 27:669–692. [PubMed: 19132917]
17. Geissmann F, Auffray C, Palframan R, Wirrig C, Ciocca A, Campisi L, Narni-Mancinelli E, Lauvau G. Blood monocytes: distinct subsets, how they relate to dendritic cells, and their possible roles in the regulation of T-cell responses. Immunol. Cell Biol. 2008; 86:398–408. [PubMed: 18392044]
18. Mizutani M, Pino PA, Saederup N, Charo IF, Ransohoff RM, Cardona AE. The fractalkine receptor but not CCR2 is present on microglia from embryonic development throughout adulthood. J. Immunol. 2012; 188:29–36. [PubMed: 22079990]
19. Saederup N, Cardona AE, Croft K, Mizutani M, Cotleur AC, Tsou CL, Ransohoff RM, Charo IF. Selective chemokine receptor usage by central nervous system myeloid cells in CCR2-red fluorescent protein knock-in mice. PLoS. One. 2010; 5:e13693. [PubMed: 21060874]
20. Bettelli E, Carrier Y, Gao W, Korn T, Strom TB, Oukka M, Weiner HL, Kuchroo VK. Reciprocal developmental pathways for the generation of pathogenic effector TH17 and regulatory T cells. Nature. 2006; 441:235–238. [PubMed: 16648838]
21. Yang Y, Weiner J, Liu Y, Smith AJ, Huss DJ, Winger R, Peng H, Cravens PD, Racke MK, Lovett-Racke AE. T-bet is essential for encephalitogenicity of both Th1 and Th17 cells. J. Exp. Med. 2009; 206:1549–1564. [PubMed: 19546248]
22. Thakker P, Leach MW, Kuang W, Benoit SE, Leonard JP, Marusic S. IL-23 is critical in the induction but not in the effector phase of experimental autoimmune encephalomyelitis. J. Immunol. 2007; 178:2589–2598. [PubMed: 17277169]
23. Pino PA, Cardona AE. Isolation of brain and spinal cord mononuclear cells using percoll gradients. J. Vis. Exp. 2011
24. Haskell CA, Hancock WW, Salant DJ, Gao W, Csizmadia V, Peters W, Faia K, Fituri O, Rottman JB, Charo IF. Targeted deletion of CX(3)CR1 reveals a role for fractalkine in cardiac allograft rejection. J Clin. Invest. 2001; 108:679–688. [PubMed: 11544273]
25. Jung S, Aliberti J, Graemmel P, Sunshine MJ, Kreutzberg GW, Sher A, Littman DR. Analysis of fractalkine receptor CX(3)CR1 function by targeted deletion and green fluorescent protein reporter gene insertion. Mol. Cell Biol. 2000; 20:4106–4114. [PubMed: 10805752]
26. Haskell CA, Cleary MD, Charo IF. Unique role of the chemokine domain of fractalkine in cell capture. Kinetics of receptor dissociation correlate with cell adhesion. Journal of Biological Chemistry. 2000; 275:34183–34189. [PubMed: 10940307]
27. Haskell CA, Cleary MD, Charo IF. Molecular uncoupling of fractalkine-mediated cell adhesion and signal transduction. Rapid flow arrest of CX3CR1-expressing cells is independent of G-

protein activation. Journal of Biological Chemistry. 1999; 274:10053–10058. [PubMed: 10187784]

28. Huang D, Shi FD, Jung S, Pien GC, Wang J, Salazar-Mather TP, He TT, Weaver JT, Ljunggren HG, Biron CA, Littman DR, Ransohoff RM. The neuronal chemokine CX3CL1/fractalkine selectively recruits NK cells that modify experimental autoimmune encephalomyelitis within the central nervous system. FASEB J. 2006; 20:896–905. [PubMed: 16675847]
29. Prinz M, Priller J, Sisodia SS, Ransohoff RM. Heterogeneity of CNS myeloid cells and their roles in neurodegeneration. Nat. Neurosci. 2011; 14:1227–1235. [PubMed: 21952260]
30. Geissmann F, Manz MG, Jung S, Sieweke MH, Merad M, Ley K. Development of monocytes, macrophages, and dendritic cells. Science. 2010; 327:656–661. [PubMed: 20133564]
31. Thomas DM, Francescutti-Verbeem DM, Kuhn DM. Methamphetamine-induced neurotoxicity and microglial activation are not mediated by fractalkine receptor signaling. J. Neurochem. 2008; 106:696–705. [PubMed: 18410508]
32. Meucci O, Fatatis A, Simen AA, Miller RJ. Expression of CX3CR1 chemokine receptors on neurons and their role in neuronal survival. Proc. Natl. Acad. Sci. U. S. A. 2000; 97:8075–8080. [PubMed: 10869418]
33. Lauro C, Di AS, Cipriani R, Sobrero F, Antonilli L, Brusadin V, Ragozzino D, Limatola C. Activity of adenosine receptors type 1 Is required for CX3CL1-mediated neuroprotection and neuromodulation in hippocampal neurons. J. Immunol. 2008; 180:7590–7596. [PubMed: 18490761]
34. Lauro C, Cipriani R, Catalano M, Trettel F, Chece G, Brusadin V, Antonilli L, van RN, Eusebi F, Fredholm BB, Limatola C. Adenosine A1 receptors and microglial cells mediate CX3CL1-induced protection of hippocampal neurons against Glu-induced death. Neuropsychopharmacology. 2010; 35:1550–1559. [PubMed: 20200508]
35. Denes A, Ferenczi S, Halasz J, Kornyei Z, Kovacs KJ. Role of CX3CR1 (fractalkine receptor) in brain damage and inflammation induced by focal cerebral ischemia in mouse. J. Cereb. Blood Flow Metab. 2008; 28:1707–1721. [PubMed: 18575457]
36. Sabate JM, Ameziane N, Lamoril J, Jouet P, Farmachidi JP, Soule JC, Harnois F, Sobhani I, Jian R, Deybach JC, de PD, Coffin B. The V249I polymorphism of the CX3CR1 gene is associated with fibrostenotic disease behavior in patients with Crohn's disease. Eur. J. Gastroenterol. Hepatol. 2008; 20:748–755. [PubMed: 18617779]
37. McDermott DH, Halcox JP, Schenke WH, Waclawiw MA, Merrell MN, Epstein N, Quyyumi AA, Murphy PM. Association between polymorphism in the chemokine receptor CX3CR1 and coronary vascular endothelial dysfunction and atherosclerosis. Circ. Res. 2001; 89:401–407. [PubMed: 11532900]
38. Apostolakis S, Baritaki S, Kochiadakis GE, Igoumenidis NE, Panutsopulos D, Spandidos DA. Effects of polymorphisms in chemokine ligands and receptors on susceptibility to coronary artery disease. Thromb. Res. 2006
39. Apostolakis S, Amanatidou V, Papadakis EG, Spandidos DA. Genetic diversity of CX3CR1 gene and coronary artery disease: new insights through a meta-analysis. Atherosclerosis. 2009; 207:8–15. [PubMed: 19439304]
40. Stojkovic L, Djuric T, Stankovic A, Dincic E, Stancic O, Veljkovic N, Alavantic D, Zivkovic M. The association of V249I and T280M fractalkine receptor haplotypes with disease course of multiple sclerosis. J. Neuroimmunol. 2012; 245:87–92. [PubMed: 22261545]
41. Broux B, Pannemans K, Zhang X, Markovic-Plese S, Broekmans T, Eijnde BO, Van WB, Somers V, Geusens P, van der Pol S, van HJ, Stinissen P, Hellings N. CX(3)CR1 drives cytotoxic CD4(+)CD28(-) T cells into the brain of multiple sclerosis patients. J. Autoimmun. 2012; 38:10–19. [PubMed: 22123179]
42. Kruglov AA, Lampropoulou V, Fillatreau S, Nedospasov SA. Pathogenic and protective functions of TNF in neuroinflammation are defined by its expression in T lymphocytes and myeloid cells. J. Immunol. 2011; 187:5660–5670. [PubMed: 22058414]
43. Murphy CA, Hoek RM, Wiekowski MT, Lira SA, Sedgwick JD. Interactions between hemopoietically derived TNF and central nervous system-resident glial chemokines underlie

initiation of autoimmune inflammation in the brain. J. Immunol. 2002; 169:7054–7062. [PubMed: 12471141]

44. Renno T, Krakowski M, Piccirillo C, Lin JY, Owens T. TNF-alpha expression by resident microglia and infiltrating leukocytes in the central nervous system of mice with experimental allergic encephalomyelitis. Regulation by Th1 cytokines. J. Immunol. 1995; 154:944–953. [PubMed: 7814894]
45. Sriram K, Matheson JM, Benkovic SA, Miller DB, Luster MI, O'Callaghan JP. Deficiency of TNF receptors suppresses microglial activation and alters the susceptibility of brain regions to MPTP-induced neurotoxicity: role of TNF-alpha. FASEB J. 2006; 20:670–682. [PubMed: 16581975]
46. Omari KM, Dorovini-Zis K. CD40 expressed by human brain endothelial cells regulates CD4+ T cell adhesion to endothelium. J. Neuroimmunol. 2003; 134:166–178. [PubMed: 12507785]
47. Shrikant P, Chung IY, Ballestas ME, Benveniste EN. Regulation of intercellular adhesion molecule-1 gene expression by tumor necrosis factor-alpha, interleukin-1 beta, and interferon-gamma in astrocytes. J. Neuroimmunol. 1994; 51:209–220. [PubMed: 7910170]

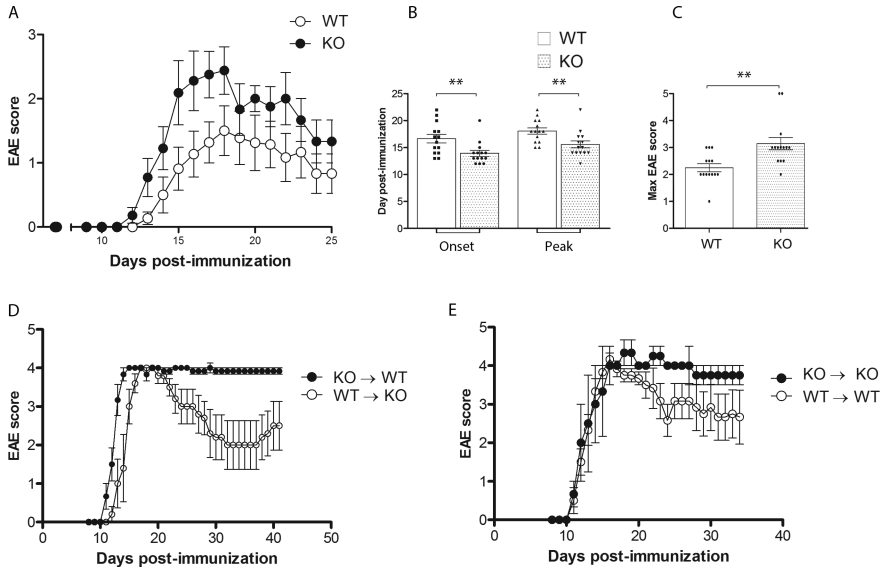

Figure 1. CX3CR1-deficient mice exhibit earlier disease onset and worse EAE disease

A) *Cx3cr1*$^{-/-}$ and *Cx3cr1*$^{+/+}$ mice were immunized with MOG_{35-55} peptide and scored daily for neurological signs. B) Days of EAE onset and peak disease. C) Maximum EAE score, $N = 14$ (*Cx3cr1*$^{+/+}$ mice) and $N = 15$ (*Cx3cr1*$^{-/-}$ mice). D) Radiation bone marrow chimeras WT → KO ($N = 8$) and KO → WT ($N = 10$) and respective controls (E) WT → WT ($N = 7$) and KO → KO ($N = 7$) were immunized with MOG_{35-55} peptide and scored daily. ** $P < 0.01$

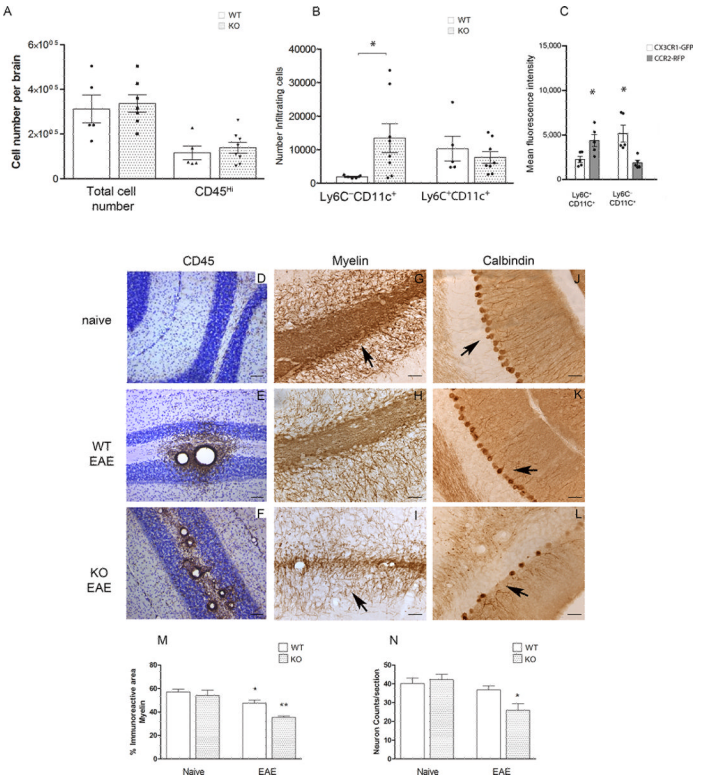

Figure 2. CX3CR1-deficient mice showed an increased accumulation of CD11c^{+} dendritic cells in CNS correlating with more severe CNS pathology

Brain mononuclear cells isolated at peak of EAE disease from *Cx3cr1*$^{GFP/+}$/*Ccr2*$^{RFP/+}$ and *Cx3cr1*$^{GFP/GFP}$/*Ccr2*$^{RFP/+}$ were separated over Percoll gradients and analyzed by flow cytometry. A) Total number of brain mononuclear cells and CD45^{Hi} infiltrating cells. (B) CD45^{Hi} infiltrating cells were gated to quantify myeloid cell subsets based on expression of CD115, Ly6C and CD11c. Open bars: *Cx3cr1*$^{GFP/+}$/*Ccr2*$^{RFP/+}$ mice with normal receptor function; shaded bars: CX3CR1-deficient *Cx3cr1*$^{GFP/GFP}$/*Ccr2*$^{RFP/+}$ mice (* P <0.05). (C) CX3CR1-GFP (open bars) and CCR2-RFP (gray bars) fluorescence intensities in monocyte subsets were compared in *Cx3cr1*$^{GFP/+}$/*Ccr2*$^{RFP/+}$ mice (* P<0.05). Values are mean ± SEM. Results are representative of two similar experiments. Brain tissues were stained with anti-CD45 antibodies (brown staining) as a marker of global inflammation and counterstained with Nissl (D-F), anti-MBP antibodies to assess demyelination (G-I) and anti-calbindin antibodies to visualize cerebellar Purkinje cells (J-L) in *Cx3cr1*$^{-/-}$ naïve (D, G, J), diseased WT (E, H and K) and *Cx3cr1*$^{-/-}$ (F, I, and L) mice. Scale bars D-F: 100 μm, G-L: 50 μm. (M) Myelin immunoreactive area, *P=0.03 between WT naïve and WT-EAE groups, **P<0.0001 between WT-EAE and KO-EAE groups. (N) Calbidin positive cells per section were counted in 4 mice per group *P=0.04 between WT-EAE and KO-EAE groups.

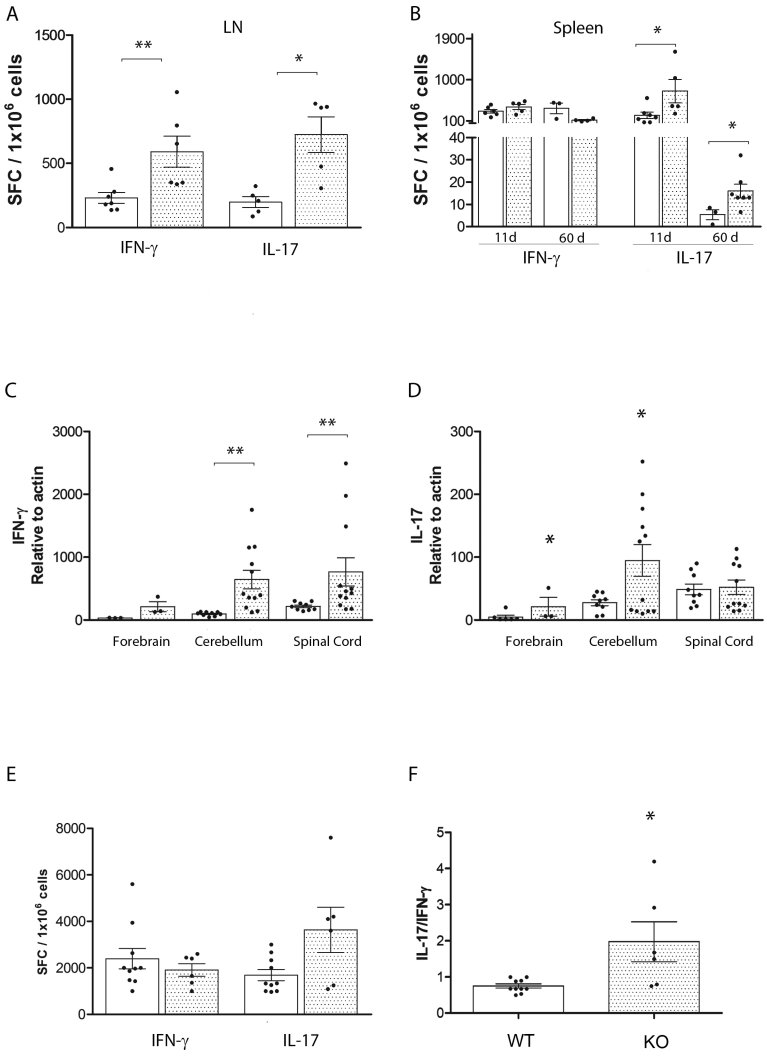

Figure 3. Cytokine expression in peripheral and CNS tissues

Lymph nodes (A) and spleen cell suspensions (B) were subjected to IFN-γ and IL-17 ELISPOT assays. Cytokine expression was measured at peak of EAE disease in brain, spinal cord (SC) and cerebellar (Cer) tissues of WT (open bars) and *Cx3cr1*$^{-/-}$ mice (shaded bars) using qRT-PCR in TaqMan assays for IFN-γ (C) and IL-17 (D). ELISPOT assays (E) and the ratio of IL-17/IFN-γ from the same sample is shown in (F). Dots on graph represent sample from an individual mouse. * $P < 0.05$, ** $P < 0.01$.

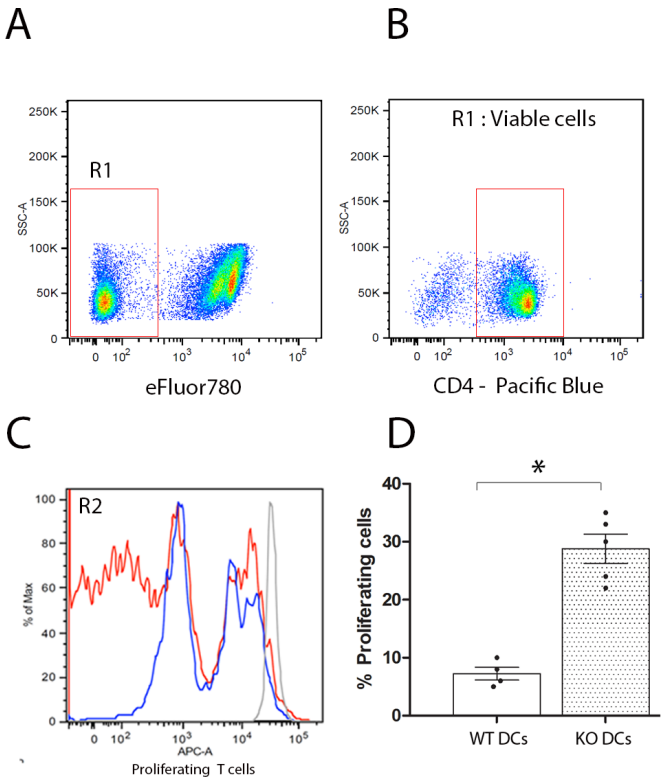

Figure 4. Effect of CX3CR1 on APCs for T cell proliferation

MOG_{35-55} primed T cells were enriched from WT mice 11 days p.i., labeled with CFSE and incubated with $CD11b^{+}CD11c^{+}$ dendritic cells isolated from WT or *Cx3cr1*$^{-/-}$ mice in presence of 20 μg/ml of MOG_{35-55} antigen. Proliferation was assessed by flow cytometry on live (A), CD4+ T cells (B). A representative experiment is shown using primed WT T cells cultured with WT (C, blue line) or *Cx3cr1*$^{-/-}$ (C, red line) dendritic cells and compared in overlapping histograms (C). Data is presented as percent of WT T cell proliferation in 3-5 different experiments in the presence of WT (D, open bar) or CX3CR1-KO dendritic cells (D, shaded bar), * $P < 0.05$.

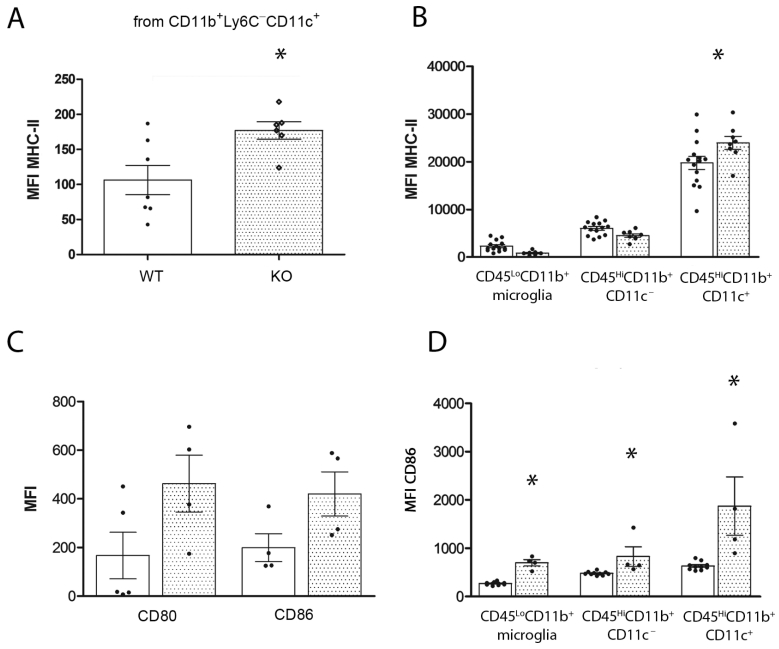

Figure 5. Effect of CX3CR1 deficiency on antigen presenting cell related molecules

Lymph nodes and brain mononuclear cells were isolated at 11 days p.i. and at peak of EAE disease respectively and analyzed for the myeloid subsets CD45, CD11b, Ly6C and CD11c by flow cytometry. Mean fluorescence intensity for MHC-II in LN (A) and brain leukocytes (B), CD80 and CD86 (C and D) were compared between WT (open bars) and KO mice (shaded bars). Each dot represents data from pooled inguinal lymph nodes from one mouse and from one brain at peak EAE disease. * $P < 0.05$.

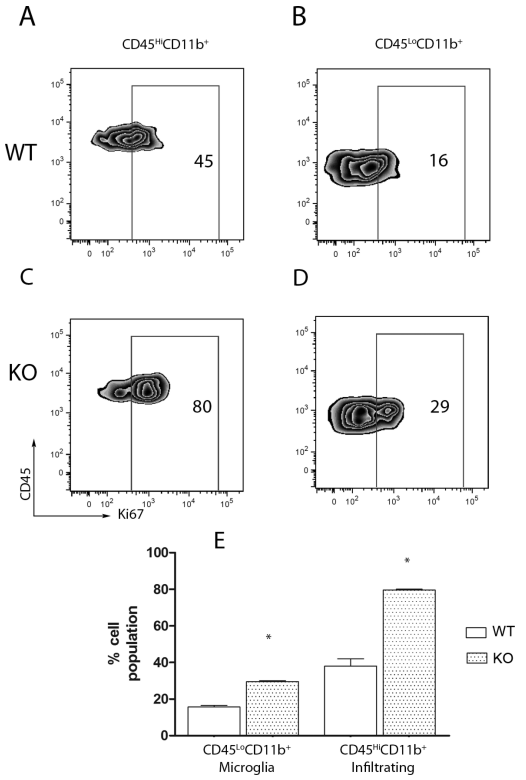

Figure 6. CX3CR1-deficient myeloid cells proliferate more readily in the CNS

Brain mononuclear cells were compared in WT (A and B) and KO mice (C and D). The proportion of proliferating Ki67^{+} cells (E) was then assessed on the gated population based on the expression of CD45 and CD11b, as CD45^{Hi}CD11b^{+} (A and C) and CD45^{Lo}CD11b^{+} (B and D).

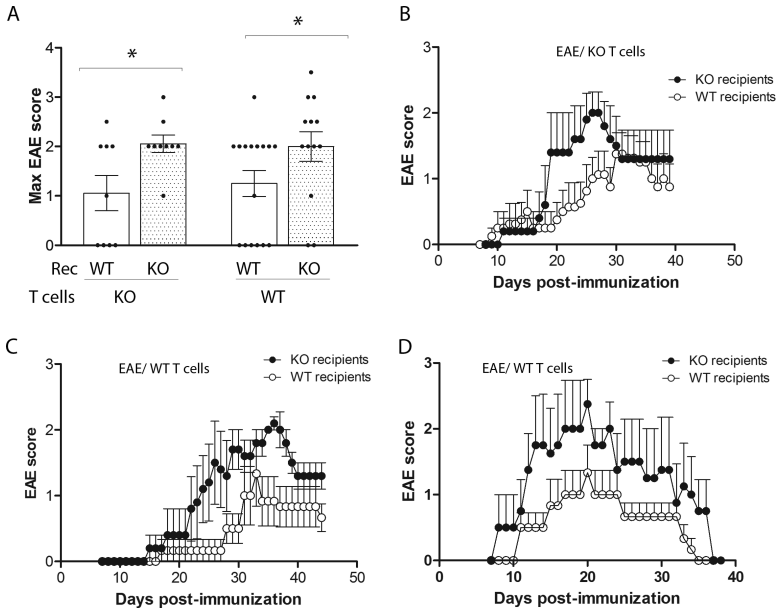

Figure 7. EAE signs were more severe in *Cx3cr1*$^{-/-}$ recipient regardless of the genotype of the T cells used for the passive transfer of EAE

Cells for adoptive transfer EAE were prepared from WT and CX3CR1-deficient mice and disease compared in WT or KO recipient mice. EAE maximum scores (A), and disease progression were monitored daily in recipients of primed KO T cells (B), two (C and D) of 3 separate experiments of recipients of WT T cells is shown. Dots in panel (A) represent an individual mouse. * $P < 0.05$.